The pH-Partition Profile of the Anti-Ischemic Drug Trimetazidine May Explain Its Reduction of Intracellular Acidosis

Frédéric Reymond,[1] Guillaume Steyaert,[2] Pierre-Alain Carrupt,[2] Didier Morin,[3] Jean-Paul Tillement,[3] Hubert H. Girault,[1] and Bernard Testa[3,4]

Received September 21, 1998; accepted February 3, 1999

Purpose. The anti-ischemic drug trimetazidine (TMZ) acts by a combination of molecular mechanisms which begin to be understood. Thus, it acts in the micromolar range to significantly reduce intracellular acidification during ischemia. To search for a possible physicochemical explanation of this phenomenon, we investigated the transfer mechanisms of the various electrical forms of this dibasic drug.

Methods. The transfer characteristics of TMZ were studied by electrochemistry at the water/1,2-dichloroethane interface. Cyclic voltammetry was used to measure the formal transfer potentials of singly and doubly protonated forms of TMZ (noted TH^+ and TH_2^{2+}, respectively) as a function of aqueous pH, and the partition coefficient of neutral TMZ (log P_T) was measured by two-phase titration.

Results. log P_T was measured to be 1.04 ± 0.06, and the acid-base dissociation constants in water were deduced to be pK_{a1}^w = 4.54 ± .02 and pK_{a2}^w = 9.14 ± 0.02. The partition coefficients of TH^+ and TH_2^{2+} were found to be respectively log $P_{TH^+}^{0\prime}$ = −3.78 ± 0.16 and log $P_{TH_2^{2+}}^{0\prime}$ = −9.84 ± 0.30, which agrees well with the charge being delocalized on two nitrogen atoms in TH^+. The pH-partition profile of TMZ was then established in the form of its ionic partition diagram, which showed that the affinity of the ions for the organic phase is pH-dependent and strongly increased by the interfacial potential.

Conclusions. This behavior suggests a physicochemical mechanism whereby efflux of protonated TMZ out of an acidified cell is facilitated, in effect exporting protons to extracellular space.

KEY WORDS: trimetazidine; lipophilicity; proton transfer; ionic partition diagram; ITIES.

INTRODUCTION

Trimetazidine (TMZ) is a dibasic compound (Fig. 1) marketed in a number of countries as a safe cellular anti-ischemic devoid of hemodynamic effects. The molecular mechanisms of its anti-ischemic effects in the myocardium and neurosensorial organs are insufficiently understood, but recent studies have revealed a variety of relevant activities (1–4).

Thus, most bioelectric activities in retina and inner ear are strongly modified by ischemia, but these deleterious effects were prevented by TMZ 10^{-6} to 10^{-5} M in blood plasma. Myocardial mitochondrial protection was evidenced in many tests, in particular in the efficacy of oral TMZ to maintain high levels of ATP despite hypoxia and calcium overload. This action is not due to an antioxidant effect (which is absent in TMZ), but to an ability to switch cellular metabolism towards preferential glucose utilization.

Another noteworthy effect of TMZ 10^{-6} M is to significantly prevent intracellular acidification during ischemia. An action on Na^+/H^+ exchange or on Na^+, K^+-ATPase was excluded, as was a simple buffering effect. To gain insight into the underlying mechanism, we used electrochemical techniques to study the pH- and potential-dependent partitioning behavior of TMZ. Our results indeed suggest a partition mechanism whereby TMZ could facilitate proton transfer from an acidic to a neutral aqueous compartment, across a lipidic compartment.

The interface between two immiscible electrolyte solutions (ITIES) is a simple model of biological membranes, and constitutes a powerful means of simulating drug transfer processes. In this respect, the water/1,2-dichloroethane (1,2-DCE) solvent system is an interesting complement to the *n*-octanol/water and alkane/water systems (5) because the partitioning between water and 1,2-DCE is mainly governed by hydrophobic interactions and by H-bonding in the water phase (6) The water/1,2-DCE system gives more weight to H-bonding than the *n*-octanol/water system, as seen also in structure-permeation relationships which consistently demonstrate the importance of H-bonding between permeant and membranes (7,8).

Electrochemical measurements in this system offer new opportunities to measure the pharmacokinetically relevant lipophilicity of ionizable solutes (9–12). Furthermore, cells function by creating a potential difference across membranes (see Mitchell's chemiosmotic model (13)). Electrochemistry has then the additional advantage of being able to investigate the interfacial movement of ions in an electric field as existing in cells. Even though there is no current/voltage source in the body, concentration differences between cytosol, intercellular space and membranes creates a potential difference of ~70 mV. This value could appear very small at first glance, but it must be remembered that the cellular membrane is only 3.5 nm thick. Thus, the potential gradient across the membrane is ~200,000 V cm^{-1}. In simple biological models such as biphasic systems,

[1] Laboratoire d'Electrochimie, Ecole Polytechnique Fédérale de Lausanne, CH-1015 Lausanne, Switzerland.

[2] Institut de Chimie Thérapeutique, Section de Pharmacie, Université de Lausanne, CH-1015 Lausanne, Switzerland.

[3] Laboratoire de Pharmacologie, Faculté de Médecine Paris XII, F-94010 Créteil, France.

[4] To whom correspondence should be addressed. (e-mail: bernard.testa@ict.unil.ch)

ABBREVIATIONS: *A*, area of the interface; C, intracellular compartment; c_I, concentration of the ion I; D_I^w, diffusion coefficient of I in the water phase; *diff*(log $P_{I-N}^{0\prime}$), logarithmic difference between the partition coefficients of an ionic and the neutral form of a compound; E, extracellular compartment; *E*, applied potential difference; $E_I^{1/2}$, observed half-wave transfer potential of I; *F*, Faraday constant; I_{peak}^{FWD}, maximum forward peak current; K_C, concentration ratio between TH^+ and T in compartment C; K_T^{CE}, transmembrane equilibrium constant for T; M, hydrophobic membrane; P_I, partition coefficient of I; $P_I^{0\prime}$, formal partition coefficient of I; pK_a^o, dissociation constant in the organic phase; pK_a^w, dissociation constant in the aqueous phase; *R*, gaz constant; *T*, temperature; T, neutral form of trimetazidine; TH^+, singly protonated form of trimetazidine; TH_2^{2+}, doubly protonated form of trimetazidine; z_I, charge of I; ΔE_{ref}, reference electrode-electrolyte potential difference; $\Delta_o^w\phi$, Galvani potential difference between the phases *w* and *o*; $\Delta_o^w\phi_I^0$, standard transfer potential of I; $\Delta_o^w\phi_I^{0\prime}$, formal transfer potential of I; $\Delta_o^w\phi_{peak}$, potential difference between the forward and the reverse peak current; $\Delta G_{tr,I}^{0,w\to o}$, standard Gibbs energy of transfer from water to oil; *v*, rate of the potential sweep.

0724-8741/99/0500-0616$16.00/0

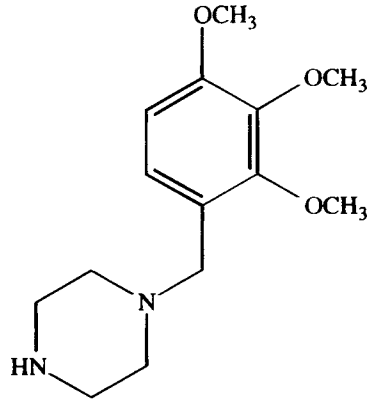

Fig. 1. Structure of trimetazidine (neutral form).

the potential is distributed over a much larger distance. Although the absolute values of the applied potential differences in biomimetic systems are much larger than the transmembranar potentials existing *in vivo*, they are not out of the range of *in vivo* potential gradients.

Finally, when an aqueous solution is brought into contact with an immiscible phase such as 1,2-DCE, the various electrical species are spontaneously distributed between the two phases. The partition of the neutral species depends primarily on the nature of the solvents, whereas that of the ionic species depends at the same time on the Galvani potential difference across the interface, on the acid-base equilibria, on the pH of the aqueous phase and on the lipophilicity of the neutral species (10). Coupled with one of the conventional methods used to determine the partition coefficient of neutral compounds, cyclic voltammetry was used here to determine the transfer mechanisms of the various ionic forms of trimetazidine (TMZ) and to assess their respective lipophilicity. These results were then used to interpret the transport behavior of TMZ in the body and to relate its physicochemical properties to some of its biological activities.

THEORETICAL BACKGROUND

The partition of ionizable solutes in biphasic systems depends on all the acid-base equilibria and also on the Galvani potential difference across the two phases (noted $\Delta_o^w\phi$) (10). Indeed, the distribution of charged species at thermodynamic equilibrium is described by the Nernst equation for the ITIES:

$$\Delta_o^w\phi = \Delta_o^w\phi_I^0 + \frac{RT}{z_I F}\ln\left(\frac{a_I^o}{a_I^w}\right) = \Delta_o^w\phi_I^{0\prime} + \frac{RT}{z_I F}\ln\left(\frac{c_I^o}{c_I^w}\right) \quad (1)$$

where a_I and c_I stand for the activity and, respectively, for the concentration of the ion I, z_I for the charge, w for the aqueous phase, o for the organic phase, $\Delta_o^w\phi_I^0$ for the standard transfer potential and $\Delta_o^w\phi_I^{0\prime}$ for the formal transfer potential of the ion I. The Galvani potential difference is the difference between the inner potentials of the two adjacent phases. It is equal to zero when there is no accumulation of charges at the interface. When positive, the aqueous phase is positively charged (accumulation of cations and/or depletion of anions) and the organic phase is negative. $\Delta_o^w\phi$ is distributed between two back-to-back diffuse Gouy-Chapman layers. The thickness of these two back-to-back space charged regions is of the order of 10 to 100 nm depending on the ionic strength of the two electrolyte solutions.

Moreover, $\Delta_o^w\phi_I^0$ is in fact the standard Gibbs energy of transfer ($\Delta G_{tr,I}^{0,w\rightarrow o}$) expressed in a potential scale, and these two quantities are simply related by:

$$\Delta_o^w\phi_I^0 = \frac{\Delta G_{tr,I}^{0,w\rightarrow o}}{z_I F} \quad (2)$$

The standard transfer potential can be understood as a Gibbs energy of transfer normalized by the charge, and it accounts for the difference of solvation in the two adjacent phases (14). As discussed later, $\Delta_o^w\phi_I^0$ is a more relevant parameter than $\Delta G_{tr,I}^{0,w\rightarrow o}$ to estimate the lipophilicity of an ionic species.

Upon variation of $\Delta_o^w\phi$, the thermodynamic equilibrium is displaced, and a certain time is needed to reach a new equilibrium state. However, for reversible (*i.e.* kinetically fast) ion transfer controlled by diffusion at the interface, it can be estimated that the equilibrium is instantaneous, so that Eq. 1 is valid whatever the rate of the potential sweep, and it can be rewritten in terms of partition coefficients:

$$\begin{aligned}\log P_I &= \frac{z_I F}{RT\ln 10}(\Delta_o^w\phi - \Delta_o^w\phi_I^{0\prime}) \\ &= \frac{z_I F}{RT\ln 10}\Delta_o^w\phi - \frac{\Delta G_{tr,I}^{0\prime,w\rightarrow o}}{RT\ln 10} \\ &= \log P_I^{0\prime} + \frac{z_I F}{RT\ln 10}\Delta_o^w\phi\end{aligned} \quad (3)$$

where P_I is the partition coefficient of I and $P_I^{0\prime}$ its formal partition coefficient (*i.e.* its partition coefficient when $\Delta_o^w\phi = 0$).

Contrary to charged species, the partition coefficient of a neutral species, P_N, is a unique quantity related to its standard Gibbs energy of transfer $\Delta G_{tr,N}^{0,w\rightarrow o}$ by:

$$\log P_N = \log\left(\frac{a_N^o}{a_N^w}\right) = -\frac{\Delta G_{tr,N}^{0,w\rightarrow o}}{RT\ln 10} \quad (4)$$

Thus, aqueous pH, $\Delta_o^w\phi$ and $\log P_N$ influence the nature and the amount of each species in both phases. At the ITIES, no redox reaction occurs upon application of a Galvani potential difference between the two phases, and the current resulting from a potential sweep is due to a flux of ions across the interface. It can easily be shown that the aqueous bulk concentration of the transferring species c_I^{w*} is related to the maximum forward peak current I_{peak}^{FWD} by the *Randles-Sevcik* equation (15):

$$I_{peak}^{FWD} = 0.4463\, z_I F A\, c_I^{w*}\left(\frac{z_I F}{RT}\right)^{1/2}(vD_I^w)^{1/2} \quad (5)$$

where A is the area of the interface, D_I^w the diffusion coefficient of I in the water phase and v is the rate of the potential sweep.

MATERIALS AND METHODS

Trimetazidine (1-(2,3,4-trimethoxybenzyl)piperazine) was kindly donated by the Institut de Recherches Internationales Servier (*IRIS*, F) and was of pharmaceutical grade. The aqueous phase was deionized water (Milli-QSP reagent water system, *Millipore*) with LiCl (*Fluka*, CH) as aqueous electrolyte, and the pH was adjusted to the desired value by addition of HNO_3 or LiOH (*Fluka*). The organic phase was 1,2-dichloroethane (1,2-DCE) of the highest available purity (*Merck*, G) with bis

(triphenylphosphoranylidene) ammonium tetrakis(4-chlorophenyl)borate (BTPPATPBCl) as organic supporting electrolyte. As 1,2-DCE is a suspected carcinogen (16), it was handled with all necessary precautions to avoid inhalation and skin contact. 1 mM TMZ was preliminarily dissolved in the aqueous phase and the experiments were carried out at room temperature (23 ± 2°C). The transfer of TMZ at the water/1,2-DCE interface was studied by cyclic voltammetry using the following electrochemical cell:

$$\mathrm{Ag|AgCl|}\begin{array}{c}\text{10mM LiCl}\\ \text{1mM BTPPACl}\end{array}\left|\begin{array}{c}\text{10mM}\\ \text{BTPPATPBCl}\end{array}\right\|\begin{array}{c}\text{1mM TMZ}\\ \text{10mM LiCl+HNO}^{3}\\ \text{or LiOH to desired pH}\end{array}\Bigg|\ \mathrm{AgCl|Ag'}$$

BTPPA$^+$ *ion selective electrode* (RE1)	1,2-DCE	water	*aqueous reference electrode* (E2)
←——→	←——→	←——→	←——→

The electrochemical apparatus was a home-made four electrode potentiostat with ohmic drop compensation. The other details of the electrochemical measurements have been described elsewhere (10). In this paper, an increase of potential renders the aqueous phase more positive with respect to the organic phase, and the flow of positive charge from the water to the 1,2-DCE phase is taken as the positive current. The transfer of trimetazidine was studied between pH 1 and 11, and it has been verified that the phase in which TMZ was preliminarily dissolved was irrelevant.

The applied potential difference E is defined as the terminal potential of the aqueous reference electrode referred to the terminal potential of the organic phase reference electrode, and it is related to the Galvani potential difference by:

$$E = \Delta_o^w\phi + \Delta E_{ref} \tag{6}$$

where ΔE_{ref} depends strongly on the nature of the two reference electrodes, so that E refers only to the electrochemical cell used, and represents a totally arbitrary scale. Thus, few drops of 10 mM tetramethyl ammonium chloride (TMACl) were added to the water phase after each experiment in order to reference all the half-wave potentials, $E_I^{1/2}$, deduced from the voltammograms. Since the formal transfer potential of TMA^+ in the absolute Galvani potential difference scale can be estimated ($\Delta_o^w\phi_{TMA^+}^{0\prime} = 160$ mV (17)) using an extra-thermodynamic assumption such as the tetraphenylarsonium tetraphenylborate (TATB) scale (18), the measured half-wave potentials $E_I^{1/2}$ can be transposed to the absolute scale by applying the following relationship:

$$E_I^{1/2} - \Delta_o^w\phi_I^{0\prime} = E_{TMA^+}^{1/2} - \Delta_o^w\phi_{TMA^+}^{0\prime} \tag{7}$$

As cyclic voltammetry cannot be applied to uncharged compounds, the partition coefficient of neutral TMZ in water/1,2-DCE was measured by pH-metric two phase titration (19, 20) (PCA101, *Sirius Analytical Instruments*, UK) and was determined to be $\log P_T = 1.04 \pm 0.06$. The acid-base equilibrium constants of TMZ in water were also measured by this method and were found to be: $pK_{a1}^w = 4.54 \pm 0.02$ and $pK_{a2}^w = 9.14 \pm 0.02$.

RESULTS AND DISCUSSION

The solubility of neutral TMZ (noted T) is very low in aqueous solution, but it can form soluble singly protonated (TH^+) or doubly protonated (TH_2^{2+}) species in acidic solution. Upon application of a Galvani potential difference across the ITIES, both TH_2^{2+} and TH^+ can transfer from water into the organic phase; the acid-base equilibria are thus modified in the vicinity of the interface, and a concentration gradient is established leading to a flux of ion diffusing from the bulk across the interface. The aqueous pH drastically influences the transfer, and electrochemistry at the ITIES is a powerful tool to demonstrate it.

Cyclic Voltammograms and Physicochemical Parameters

The half-wave transfer potentials of the two cationic forms of trimetazidine were determined by cyclic voltammetry as a function of the aqueous pH, as shown in Fig. 2 for several experiments achieved with the above electrochemical cell.

These results show that four types of voltammograms can be differentiated depending on pH. Up to pH 2, only one current wave was observed within the available potential window. With respect to the acid-base equilibria, TMZ is mainly in its diprotonated form at such pH (pK_{a1}^w was measured to be 4.5 ± 0.02), and the current can be attributed to the transfer of TH_2^{2+} from water to 1,2-DCE on the forward scan and to the opposite process on the reverse scan. The measured half-wave potential was constant in this pH range and $\Delta_o^w\phi_{TH_2^{2+}}^{0\prime}$ deduced from Eqn. 7 is 291 ± 9 mV. The shape of the voltammogram indicates that this transfer was diffusion-controlled which implies that the ion transport across the interface was very fast. The reversibility of the transfer is demonstrated by the linear dependence of the maximum peak current on the square root of the sweep rate as predicted by the *Randles-Sevcik* equation (Eqn. 5), by the position of the forward and reverse peaks which is independent of the scan rate, and by the value of ~30 mV for the potential difference between the forward and the reverse peak current (peak-to-peak separation $\Delta_o^w\phi_{peak}$) which should be $RT/zF = 59/z$ mV at 25°C.

Between pH 2 and 4.5, a second current wave appeared at less positive potentials than that due to TH_2^{2+}, and it was generated by a flux of TH^+ across the interface. Both waves were reversible, but the peak-to-peak separation corresponded in both cases to the transfer of a monocharged ion since at pH 2.9 $\Delta_o^w\phi_{peak}$ was 58 and 66 mV for the first and second peak, respectively. Furthermore, the half-wave potentials were not constant in this pH range: when pH increased, the wave due to TH^+ transfer was shifted to smaller potentials, whereas $\Delta_o^w\phi_{TH_2^{2+}}^{1/2}$ increased. At pH 4.0, Fig. 2 shows that the first wave was slightly displaced to the left with respect to that obtained at pH 2.9 and that the second peak blended in the positive end of the potential window. This can be explained by the mechanisms governing the transfer at such pH, as discussed below in the mechanistic interpretation of the ionic partition diagram of TMZ.

From pH 4.5 to 9, only one current wave was observed within the potential window. It resulted from the transfer of TH^+ across the water/1,2-DCE interface since it was the only charged species present at such pH values (pK_{a2}^w was measured to be 9.14 ± 0.02). The maximum forward peak current followed the bulk concentration of TH^+ all over this pH range, the half-wave potential remained constant and $\Delta_o^w\phi_{TH^+}^{0\prime}$ was calculated to be 162 ± 9 mV.

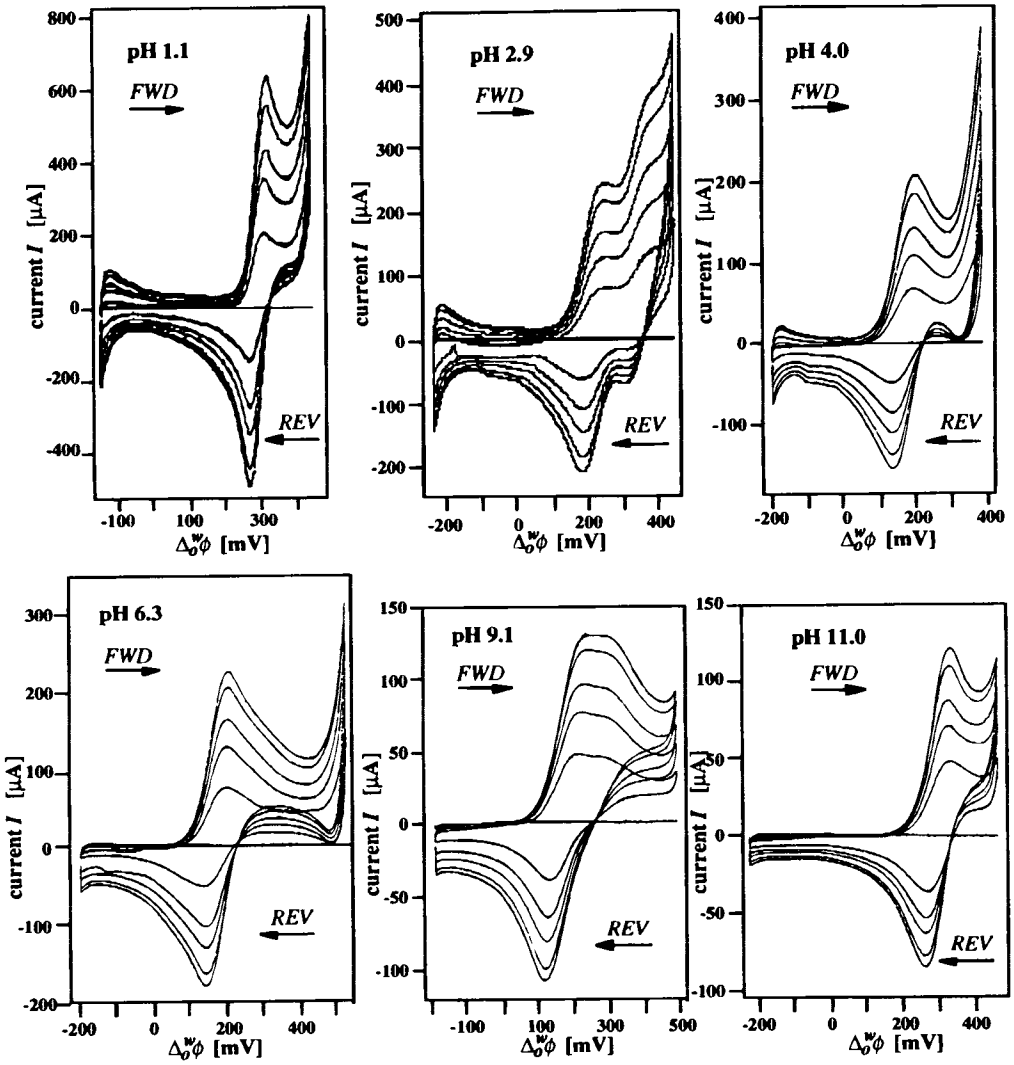

Fig. 2. Typical cyclic voltammograms obtained at various values of aqueous pH for the transfer of trimetazidine at the water/1,2-DCE interface. The potential scan rate v is 10, 30, 50, 80 and 100 mVs^{-1}; the forward scan (fwd) is from left to right (upper part of the curves) and the reverse scan (rev) from right to left. The data are already transposed from the applied potential scale to the absolute Galvani potential scale.

Above pH = pK_{a2}^w, trimetazidine is mainly neutral and polarization of the interface cannot lead to the transfer of any form of TMZ. However, a third wave appeared on the voltammograms in Fig. 2 which corresponded to the transfer of a monocharged species ($\Delta_o^w\Phi_{peak}$ is always ~60 mV). The transfer reaction was reversible and the measured half-wave potential increased by ~60 mV per pH unit. It will be shown below that this transfer wave is due to the transfer of a proton facilitated by neutral trimetazidine present in the organic phase.

It must also be pointed out that the current intensity varied with the aqueous concentration of protons. When pH approached pK_{a1}^w, the current due to TH^+ transfer increased rapidly and that due to TH_2^{2+} diminished even faster. This was due to the changing ionic composition of the aqueous phase upon pH increases, and the measured variations of the maximum forward peak currents are in good agreement with the fact that I_{peak}^{FWD} varies with $(z)^{3/2}$ (see Eqn. 5). Indeed, at v = 100 mVs^{-1}, Fig. 2 shows that I_{peak}^{FWD} was 598, 197 and 222 μA at pH 1.1, 4.0 and 6.3, respectively. Estimating in a first approximation that TH_2^{2+} and TH^+ have the same diffusion coefficients in water, $I_{peak}^{FWD}/(z)^{3/2}$ must only depend on the bulk concentration of the transferring species, which is in total accordance with the smaller value obtained at pH 3.96 for which $c_{TH_2^{2+}}^{w*}$ cannot be neglected. Finally, above pH = pK_{a2}^w the peak current was determined by the concentration of neutral TMZ in the organic phase and by the proton concentration in the aqueous phase. These two parameters acted in opposite directions, so that it is not surprising to obtain a constant value of I_{peak}^{FWD} in this domain of pH.

It must be stressed that the phase in which TMZ was preliminarily dissolved is irrelevant, because it partitions between the two phases as soon as they are brought into contact. Therefore, partitioning of neutral TMZ at high pH does not disturb the experiments since, as will be demonstrated below, the recorded current is due to a transfer of proton assisted by $TH^+(o)$.

In addition to the acid-base dissociation constants and the partition coefficient of TMZ measured by titration, this study

of the pH dependence of transfer allows to quantify the physicochemical parameters determining the distribution of all the species involved. These values are compiled in Table 1, and will be used to draw the ionic partition diagram of TMZ and to discuss its lipophilicity in water/1,2-DCE.

Ionic Partition Diagram

With two protonation sites, the thermodynamic cycle for the transfer of a dibase across an ITIES includes eight different species distributed over the two phases (namely, T, TH^+, TH_2^{2+} and the proton H^+). As can be deduced from the ionic partition diagram methodology (21), all these species are connected by seven boundary lines representing the equiconcentration domains of two adjacent species. In the case of $TH_2^{2+}(o)$ and $TH_2^{2+}(w)$ for instance, the equiconcentration is reached when $c^o_{TH_2^{2+}}/c^w_{TH_2^{2+}} = 1$. Thus, the logarithmic term in Eqn. 1 becomes zero, and the boundary line is given by $\Delta^w_o \phi = \Delta^w_o \phi^{0\prime}_{TH_2^{2+}}$. The same method is used to deduce the other boundary lines from the Nernst equations expressed for each ionic species and from the definition of the acid-base dissociation constants, and these lines are the geometric locus delimiting the domain of predominance of each species involved. With the experimental results given in Table 1, it is straightforward to express these boundary lines numerically and to calculate their end points (see Ref. (21)). The results obtained are displayed in Fig. 3 which shows the ionic partition diagram of trimetazidine in water/1,2-DCE at 25°C.

As the partition of a neutral species is neither pH- nor potential-dependent, only T(w) is chosen to draw the ionic partition diagram (see Ref. (21) for details). The value of the partition coefficient is incorporated in the predominance domain of neutral TMZ in Fig. 3 so as to keep in mind that T(w) and T(o) are present in a proportion given by their $\log P_N$. In the present case, the concentration of neutral TMZ is always ~ 10 times larger in 1,2-DCE than in water. Otherwise, lines a and b show the limits of the experimental domain for the electrochemical cell used, of which the potential window was limited by the transfer of Cl^- and Li^+ at low and, respectively, high potentials ($\Delta^w_o \phi^0_{Cl^-} = 470$ mV (22) and $\Delta^w_o \phi^0_{Li^+} = 576$ mV (23)).

The ionic partition diagram of TMZ offers an instantaneous view of how experimental conditions influence the nature of the species in solution and their transfer. Indeed, a displacement in the ionic partition diagram generates a change of concentration of all species in both phases. When a boundary line is crossed, the predominant species changes, which implies that a reaction occurs. This reaction can be either the transfer of a species from one phase to the other or an acid-base transformation. It is shown hereafter that this representation greatly helps the interpretation of the results obtained by cyclic voltammetry.

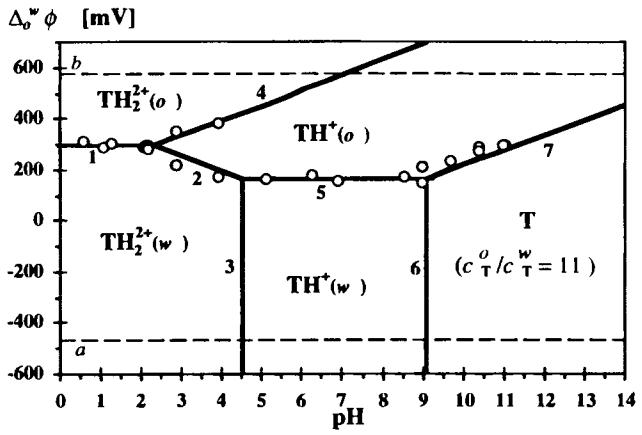

Fig. 3. Ionic partition diagram of trimetazidine at 25°C in water/1,2-DCE. The circles denote the experimental values deduced from the voltammograms, while the boundary lines (bold) are determined using the mean value of $\Delta^w_o \phi^{0\prime}_i$ given in Table 1. Lines a and b denote the experimental domain, which is limited here by the transfer of Li^+ and Cl^- at high and low potentials, respectively. The numbers differentiate the various boundary lines between two adjacent species: 1 stands for the equiconcentration between TH_2^{2+} (w) and TH_2^{2+} (o), 2 for the equiconcentration between TH_2^{2+} (w) and $TH^+(o)$, and so on.

Transfer Mechanisms

All the experimental values of the formal transfer potentials deduced from the voltammograms have been added to Fig. 3, which shows the good agreement between theory and experimental results. Indeed, the four pH domains discussed above are clearly delimited on the ionic partition diagram. Upon positive polarization of the interface at pH < 2, the boundary between the predominance domains of $TH_2^{2+}(w)$ and $TH_2^{2+}(o)$ (line 1 in Fig. 3) is crossed, and doubly charged trimetazidine simply transfers from water into 1,2-DCE. At pK^w_{a1} < pH < pK^w_{a2}, similar considerations apply for TH^+ which is also forced to transfer into the organic phase upon polarization.

Outside these two pH domains, the polarization of the interface generates unexpected phenomena due to the equilibria linking all species. The proton plays a fundamental role in these regions, and the mechanisms governing transfer can be deduced from the nature of the two corresponding predominance domains. To facilitate the discussion, all the reactions that take

Table 1. Physicochemical Parameters Determining the Thermodynamic Equilibria of Trimetazidine at the Water/1,2-DCE Interface

	$\Delta^w_o \phi^{0\prime}_i$ [mV]	$\Delta G^{0\prime,w\to o}_{tr,i}$ [kJmol^{-1}]	$\log P^{0\prime}_i$	$diff(\log P^{0\prime}_{i-N})^{a)}$	$pK^{w\,b)}_a$	$pK^{o\,c)}_a$
TH_2^{2+}	291 ± 9	56.2 ± 1.7	−9.84 ± 0.30	−10.88 ± 0.31	4.54 ± 0.02	6.85 ± 0.38[d)]
TH^+	162 ± 9	15.6 ± 0.9	−2.74 ± 0.15	−3.78 ± 0.16	9.14 ± 0.02	14.77 ± 0.24[e)]

[a] Log P_T is 1.04 ± 0.06 and was measured by Sirius pH-metric two phase titration.
[b] Measured by Sirius pH-metric two phase titration.
[c] Calculated with $\Delta^w_o \phi^{0\prime}_{H^+} = 549 \pm 10$ mV (30).
[d] pK^o_a is defined as the negative logarithmic value of the dissociation constant in the organic phase with respect to the proton concentration in the organic phase and it is deducted from: $pK^o_{a1} = pK^w_{a1} + \log P^{0\prime}_{TH_2^{2+}} - \log P^{0\prime TH} - \log P^{0\prime}_{H^+}$.
[e] Deduced from: $pK^o_{a2} = pK^w_{a2} + \log P^{0\prime}_{TH^+} - \log P_T - \log P^{0\prime}_{H^+}$ (see Ref. (10)).

place with TMZ at the water/1,2-DCE interface are schematically shown in Fig. 4.

Boundary line 2 (Fig. 3 and 4) shows that between pH 2 and 4.5, doubly charged TMZ in the aqueous phase has to loose a proton to cross the interface, since, upon positive polarization of the interface, we pass from the predominance domain of $TH_2^{2+}(w)$ to that of $TH^+(o)$. The singly charged species needs a supplementary input of energy to recover its second proton and $TH^+(o)$ acts then as an ionophore for the proton. The transfer proceeds by Interfacial Complexation (TIC mechanism) (24) and this explains why a second wave appeared on the corresponding voltammogram in Fig. 2. The overall mechanism can thus be summarized as follows:

$$TH^+(w) + H^+(w) \rightleftarrows TH_2^{2+}(w) \text{ dissociation equilibrium} \quad (8)$$

$$TH^+(w) \rightleftarrows TH^+(o) \text{ first peak, transfer of } TH^+ \quad (9)$$

$$TH^+(o) + H^+(w) \rightleftarrows TH_2^{2+}(o) \text{ second peak, transfer of } H^+ \quad (10)$$

Such a mechanism also agrees with the fact that I_{peak}^{FWD} is much smaller at pH 2.9 than at pH 1.1, and that the two recorded peaks were due to a singly charged species crossing the interface. It is also of interest to note that the smaller the concentration of $TH_2^{2+}(w)$, the smaller the potential needed to form $TH^+(o)$ and the larger the supplementary energy required for $TH^+(o)$ to facilitate the transfer of a proton. This result confirms that the affinity of an ionic species for the organic phase is both pH- and potential-dependent (see Eq. 3) and that there is only a well-defined domain of pH where its partition coefficient can be considered constant.

Above pH = pK_{a2}^w, the predominant species were $T(o)$ and $TH^+(o)$ at low and, respectively, high potentials. To pass from one domain to the other, neutral TMZ needs to protonate, and, as already observed in other experiments (11,21,25), the sweeping of potential displaces the thermodynamic equilibria so strongly that $T(o)$ can in turn act as a protonophore. In this manner, the current observed in Fig. 2 at pH 11 follows also from the passage of a proton across the interface.

Lipophilicity

As expected, neutral trimetazidine is the most lipophilic species since Table 1 shows that it has the largest partition coefficient. As generally noted, the hydration energy of charged species is more negative than their solvation energy in the organic phase, so that they are better stabilized in water than in the organic phase. By contrast, neutral TMZ requires energy to pass from 1,2-DCE into water.

The ionic partition diagram also illustrates the lipophilicity of the different species present. As shown by Eq. 2, the larger the formal transfer potential of an ion, the larger the energy required to let it cross the water/1,2-DCE interface. Consequently, TH_2^{2+} is significantly less lipophilic than TH^+, since the boundary line corresponding directly to the transfer of TH_2^{2+} (line 1 in Fig. 3 and 4) is positioned at a larger potential than that representing the transfer of TH^+ (line 5).

As discussed above, the log $P_I^{0\prime}$ parameter can be slightly confusing when comparing the lipophilicity of ions of different charges. In the present case for instance, the value of −9.84 for log $P_{TH_2^{2+}}^{0\prime}$ suggests that the doubly charged form of TMZ can never transfer into the organic phase and hence that it will never cross biological membranes. However, as the movement of ions in biology is determined by their electrochemical potential, the driving force for permeation of ions into biological barriers by passive diffusion is the transmembrane Galvani potential difference. Being normalized by the charge, the formal ion transfer potential $\Delta_o^w\phi_I^{0\prime}$ is thus the key parameter of its lipophilicity. Indeed, for a given electrical work, the water/organic phase distribution of singly and doubly charged ions is drastically different. As shown in this study, if the transfer of TH_2^{2+} necessitates ~3.6 times more energy than that of TH^+, the Galvani potential difference required for this process is only ~1.8 times larger for TH_2^{2+} than for TH^+ (see Table 1). In other terms, to reach the equiconcentration in the two adjacent phases, a singly charged ion with the same log $P_I^{0\prime}$ as TH_2^{2+} would require twice the potential needed by TH_2^{2+} (*i.e.* 582 mV). Consequently, even if both log $P_I^{0\prime}$ are equal, these two ions

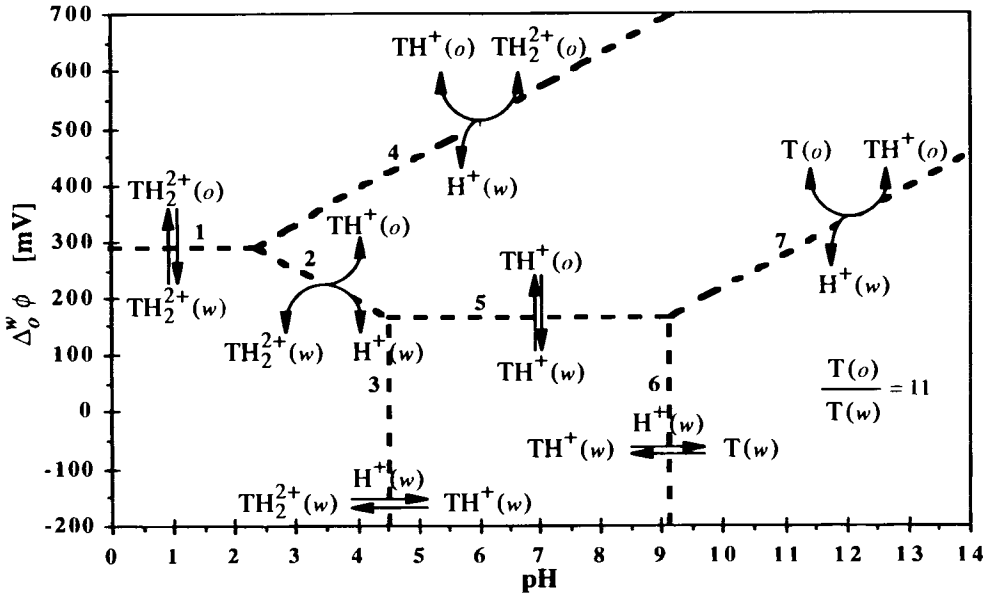

Fig. 4. Schematic transfer mechanisms of the various forms of trimetazidine at the water/1,2-DCE interface. The number are the same as in Fig. 3.

do not have the same affinity for the organic phase. Due to their higher charge, the doubly charged ions will be more efficiently forced towards the organic phase under the influence of polarization. The formal transfer potential scale is thus more informative than the formal partition coefficient scale to interpret the lipophilicity of ions and to appreciate their capability to permeate into membranes.

The partition coefficient difference between an ionic and the neutral form of a compound (defined as $diff(\log P^{0\prime}_{I-N}) = \log P^{0\prime}_{I} - \log P_N$) is a recently introduced parameter to assess the effect of charge on lipophilicity (14,26). With TMZ, protonation of the neutral species generates a relatively small decrease in lipophilicity: $diff(\log P^{0\prime}_{TH^+-T})$ is -3.78, whereas the common value of -5 is generally obtained with monocharged species at the water/1,2-DCE interface. At first glance, this small shift cannot be understood on the simple basis of its chemical structure, since only a conformational change can slightly stabilize the charge by internal conjugation with the *ortho* oxygen atom. The nitrogen atoms are positioned in very similar environments, so that they have approximately the same basicity. Moreover, the piperazine ring can adopt a "boat" conformation which markedly decreases the distance between the two nitrogens. In TH^+, the proton can pass from one nitrogen atom to the other. This induces an important delocalization of the charge which greatly favors solvation in an organic phase where no H-bond stabilization is possible (14). However, this effect disappears upon diprotonation. TH_2^{2+} is extremely hydrophilic in comparison to T and TH^+, since Table 1 shows that $diff(\log P^{0\prime}_{TH_2^{2+}-T}) = -10.88$. In this case, the two charges cannot delocalize, and as they are close from each other, they induce a very strong electrostatic field which is very difficult for 1,2-DCE to stabilize. Furthermore, the water molecules forming the first solvation shell are strongly attracted by the doubly charged species, which explains why the formal transfer potential of TH_2^{2+} is very large. Thus, upon transfer from water into 1,2-DCE, the destruction of the aqueous solvation shell and its replacement with organic solvent molecules necessitates a very large amount of energy, and the affinity of TH_2^{2+} for the organic phase is then very low.

The difference in lipophilicity between charged and neutral forms of an ionizable drug can have dramatic consequences for its pharmacokinetic phase (27–29), and it will be shown below how the ionic forms of trimetazidine can affect its membrane permeation and thus its pharmacological effects.

Relations Between Physicochemical and Pharmacological Properties

Administered orally, trimetazidine is first liberated in the stomach, which greatly favors its dissolution since it is doubly charged around pH 1. To pass into blood, trimetazidine has yet to cross several biological barriers. The ionic partition diagram suggests that this step would require energy, since, at zero potential and low pH, the doubly charged species in the aqueous phase dominates. Furthermore, as only TH_2^{2+} exists at very low pH, trimetazidine needs to leave the stomach to yield TH^+. Given that the formal Gibbs energy of transfer diminishes when pH increases, this will greatly facilitate the passage into membranes (indeed, $\log P^{0\prime}_{TH_2^{2+}}$ and $\log P^{0\prime}_{TH^+}$ are separated by ~7 units!).

As for the pharmacodynamically active species acting on hypothetical target sites, we can simply deduce from the ionic partition diagram that the monoprotonated species predominates at physiological pH. High- and low-affinity binding sites for TMZ have been found in mitochondrial membranes (3), but the species binding to these sites, and their pharmacodynamic relevance, remain to be elucidated.

The problem we now examine is a possible relation between the ionic partition diagram of TMZ (Fig. 4) and its documented capacity to prevent intracellular acidosis during ischemia. A traditional and a more recent view of passive membrane permeation are presented in Fig. 5A and 5B, respectively. Assuming no permeation for TH^+, its concentration in the two compartments will depend only on pK_a and on the two pH values (Fig. 5A). When TH^+ can permeate (Fig. 5B), its

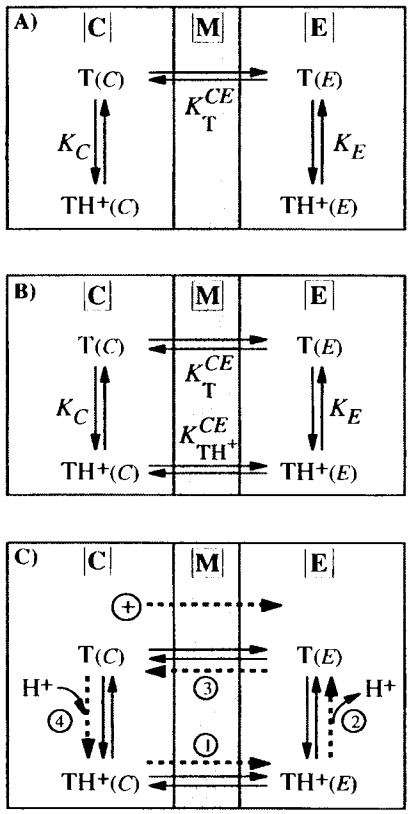

Fig. 5. Permeation mechanism for passive drug transfer from an intracellular compartment C to an extracellular compartment E separated by a membrane M. A) Scenario 1: The traditional view of passive drug transfer across membranes, with no permeation of the cationic form TH^+ of the drug T. Assuming that $pK_a = 9$ and that pH is 6 in C and 7 in E, $K_C = c^C_{TH^+}/c^C_T = 1000/1$, $K_E = c^E_{TH^+} / c^E_T = 100/1$, since $K^{CE}_T = c^C_T/c^E_T$ must obviously be 1. B) Scenario 2: A more recent view of drug transfer across membranes, with the cationic form also permeating. Assuming the same conditions as in A), the equality $K^{CE}_T = 1 = K^{CE}_{TH^+}$ must be met, which in effect decreases $c^C_{TH^+}$ and increases $c^E_{TH^+}$ until a new equilibrium is reached. C) Scenario 3: An interfacial potential difference is created between C and M. This will drive $TH^+(C)$ into M, from where it will escape into E (step 1). The excess of $TH^+(E)$ will deprotonate according to pK_a (step 2). Equilibrium between T(*E*) and T(*C*) will tend to be restored in step 3. Equilibrium between T(*C*) and $TH^+(C)$ will tend to be restored in step 4. A cycle is created which effectively transfers H^+ from C to E.

concentration in an intracellular compartment (noted C) must be equal to that in an extracellular compartment (E) at equilibrium. Indeed, as $P_{TH^+}{}^{+}$ is constant in absence of interfacial potential, $K_T^{CE} = P_{TH^+}^{EM} / P_{TH^+}^{CM} = 1$ and $c_{TH^+}^{C} = c_{TH^+}^{E}$ must exist at equilibrium. This condition is obtained by $c_{TH^+}^{C}$ decreasing (apparent decrease of pK_a in C) and $c_{TH^+}^{E}$ increasing (apparent increase of pK_a in E) until equilibrium is reached, which induces a slight displacement of the dissociation equilibria in both C and E. The capacity of such a reaction to compensate for acidosis in C should be very limited.

The picture changes when an interfacial potential difference is created, as resulting from fast acidification due to ischemia. The results of this study reveal that such a potential difference will push TH^+ (c) into the membrane, thus further and strongly increasing its lipophilicity (Fig. 5C). From here, TH^+ will escape into E and deprotonate according to pK_a. If E is an open compartment (*e.g.* extracellular fluid or blood), the excess of protons will be eliminated. The cycle continues with T permeating into C (since $c_T^E > c_T^C$), and T(c) reforming TH^+ (c). The cycle will carry on as long as the interfacial potential difference persists, and this is in analogy to "counter transport" in which solutes can be transported against their concentration gradients.

CONCLUSIONS

Cyclic voltammetry at the ITIES has been shown to be a relevant technique to assess the physicochemical parameters describing the distribution of the various forms of trimetazidine in the water/1, 2-DCE system. The partition coefficients of all forms of TMZ have been determined in the present study, and it has been shown that the rather large lipophilicity of the monoprotonated form of TMZ is due to the delocalization of the proton. The proximity of the two nitrogen atoms as well as their similar basicity favors this charge delocalization in TH^+, which weakens the induced electrostatic field and thus improves its solvation in the organic phase. This effect disappears with TH_2^{2+}, explaining its much smaller lipophilicity.

The potential-dependent lipophilicity led us to propose a mechanism of facilitated proton transfer to explain the antiacidosis effect of TMZ. The conceptual gap between biophysical conditions in cells and our physicochemical set-up is of course broad, but our model offers a plausible mechanism the pharmacological value of which is worth further assessment.

ACKNOWLEDGMENTS

P.-A. C., H. H. G., and B. T. are grateful for financial support by the *Swiss National Science Foundation*. Laboratoire d'Electrochimie is part of the European Training and Mobility Network on "Organisation, Dynamics and Reactivity at Electrified Liquid/Liquid Interfaces" (ODRELLI). The authors are indebted to Prof. Aimé Crevat (*University of Marseille*, F) and Dr. Alain Le Ridant (*IRIS*, F) for their constant interest and fruitful discussions.

REFERENCES

1. D. Salducci, A. M. Chauvet-Monges, J.-P. Tillement, E. Albengres, B. Testa, P.-A. Carrupt, and A. Crevat, Trimetazidine Reverses Calcium Accumulation and Impairment of Phosphorylation Induced by Cyclosporine A in Isolated Rat Liver Mitochondria. *J. Pharmacol. Exp. Ther.* **277**:417–422 (1996).
2. D. Lagadic-Gossmann, K. Le Prigent, and D. Feuvray, Effects of Trimetazidine on pHi Regulation in the Rat Isolated Ventricular Myocyte. *Br. J. Pharmacol.* **117**:831–833 (1996).
3. D. Morin, A. Elimadi, R. Sapena, A. Crevat, P.-A. Carrupt, B. Testa, and J.-P. Tillement, Evidence for the Existence of [^{3}H]Trimetazidine Binding Sites Involved in the Regulation of the Mitochondrial Permeability Transition Pore. *Br. J. Pharmacol.* **123**:1385–1394 (1998).
4. E. Albengres, J.-P. Tillement, H. Le Louet, and D. Morin, Trimetazidine: Experimental and Clinical Update Review. *Cardiovascular Drug Reviews* (in press).
5. N. El Tayar, B. Testa, and P.-A. Carrupt, Polar Intermolecular Interactions Encoded in Partition Coefficients: An Indirect Estimation of Hydrogen-Bond Parameters of Polyfunctional Solutes. *J. Phys. Chem.* **96**:1455–1459 (1992).
6. G. Steyaert, G. Lisa, P.-A. Carrupt, B. Testa, F. Reymond, and H. H. Girault, Solvatochromic Analysis of Partition Coefficients in the Water/1,2-Dichloroethane System. *J. Chem. Soc., Faraday Trans.* **93**:401–406 (1997).
7. M. S. Roberts, W. J. Pugh, and J. Hadgraft, Epidermal Permeability-Penetrant Structure Relationships. 2. The Effect of H-Bonding Groups in Penetrants on Their Diffusion through The Stratum Corneum. *Int. J. Pharm.* **132**:23–32 (1996).
8. W. J. Pugh, M. S. Roberts, and J. Hadgraft, Epidermal Permeability-Penetrant Structure Relationships: 3. The Effect of Hydrogen Bonding Interactions and Molecular Size on Diffusion across the Stratum Corneum. *Int. J. Pharm.* **138**:149–165 (1996).
9. E. Wang, Z. Yu, and N. Li, Anaesthetic Lidocaine, and Dicaine Transfer across Liquid/Liquid Interfaces. *Electroanalysis* **4**:905–909 (1992).
10. F. Reymond, G. Steyaert, P.-A. Carrupt, B. Testa, and H. H. Girault, Mechanism of Transfer of a Basic Drug across the Water/1,2-Dichloroethane Interface: the Case of Quinidine. *Helv. Chim. Acta* **79**:101–117 (1996).
11. F. Reymond, G. Steyaert, A. Pagliara, P.-A. Carrupt, B. Testa, and H. Girault, Transfer Mechanism of Ionic Drugs: Piroxicam as an Agent Faciliting Proton Transfer. *Helv. Chim. Acta* **79**:1651–1669 (1996).
12. G. Caron, A. Pagliara, P. Gaillard, P.-A. Carrupt, and B. Testa, Ionization and Partitioning Profiles of Zwitterions: The Case of the Anti-Inflammatory Drug Azapropazone. *Helv. Chim. Acta* **79**:1683–1695 (1996).
13. P. Mitchell, Keilin's Respiratory Chain Concept and Its Chemiosmotic Consequences. *Science* **206**:1148–1159 (1979).
14. F. Reymond, P.-A. Carrupt, B. Testa, and H. H. Girault, Charge and Delocalisation Effects on the Lipophilicity of Protonable Drugs. *Chem. Eur. J.* **5**:39–47 (1999).
15. A. J. Bard, and L. R. Faulkner, *Electrochemical Methods: Fundamentals and Applications*, Wiley, New York, 1980.
16. International Program on Chemical Safety, *1,2-Dichloroethane*, Environmental Health Criteria Vol. 176. World Health Organization, Geneva, 1995.
17. T. Wandlowski, V. Marecek, and Z. Samec, Galvani Potential Scales for Water-Nitrobenzene and Water-1,2-Dichloroethane Interfaces. *Electrochim. Acta* **35**:1173–1175 (1990).
18. E. Grunwald, G. Baughman, and G. Kohnstam, The Solvation of Electrolytes in Dioxane-Water Mixtures, as Deduced from the Effect of Solvent Change on the Standard Partial Molar Free Energy. *J. Am. Chem. Soc.* **82**:5801–5811 (1960).
19. A. Avdeef, pH-Metric logP. Part 1. Difference Plots for Determining Ion-Pair Octanol-Water Partition Coefficients of Multiprotic Substances. *Quant. Struct.-Act. Relat.* **11**:510–517 (1992).
20. A. Avdeef, Assessment of Distribution-pH Profiles. In V. Pliska, B. Testa and H. van de Waterbeemd (eds.), *Lipophilicity in Drug Action and Toxicology*, VCH, Weinheim, 1996, pp. 109–139.
21. F. Reymond, G. Steyaert, P.-A. Carrupt, B. Testa, and H. H. Girault, Ionic Partition Diagrams: A Potential-pH Representation. *J. Am. Chem. Soc.* **118**: 11951–11957 (1996).
22. Y. Shao, and S. G. Weber, Direct Observation of Chloride Transfer across the Water/Organic Interface and the Transfer of Long-Chain Dicarboxylates. *J. Phys. Chem.* **100**:14714–14720 (1996).
23. Y. Shao, A. A. Stewart, and H. H. Girault, Determination

of the Half-Wave Potential of the Species Limiting the Potential Window. *J. Chem. Soc. Farad. Trans.* **87**:2593–2597 (1991).
24. Y. Shao, M. D. Osborne, and H. H. Girault, Assisted Ion Transfer at Micro-ITIES Supported at the Tip of Micropipettes. *J. Electroanal. Chem.* **318**:101–109 (1991).
25. T. Ohkouchi, T. Kakutani, and M. Senda, Electrochemical Study of the Transfer of Uncouplers across the Organic/Aqueous Interface. *Bioelectrochem. Bioenerg.* **25**:71–80 (1991).
26. A. Pagliara, P.-A. Carrupt, G. Caron, P. Gaillard, and B. Testa, Lipophilicity Profiles of Ampholytes. *Chem. Rev.* **97**:3385–3400 (1997).
27. H. Kubinyi, *QSAR: Hansch Analysis and Related Approaches*. VCH, Weinheim, 1993.
28. V. Pliska, The Role of Lipophilicity in Biological Response to Drugs and Endogenous Ligands. In V. Pliska, B. Testa and H. van de Waterbeemd (eds.), *Lipophilicity in Drug Action and Toxicology*, VCH, Weinheim, 1996 pp. 264–293.
29. D. A. Smith, B. C. Jones, and D. K. Walker, Design of Drugs Involving the Concepts and Theories of Drug Metabolism and Pharmacokinetics. *Med. Res. Rev.* **16**:243–266 (1996).
30. A. Sabela, V. Marecek, Z. Samec, and R. Fuoco, Standard Gibbs Energies of Transfer of Univalent Ions from Water to 1,2-Dichloroethane. *Electrochim. Acta* **37**:231–235 (1992).